

# Carbon Stocks Estimation in South East Sulawesi Tropical Forest, Indonesia, using Polarimetric Interferometry Synthetic Aperture Radar (PolInSAR)

La Ode Muhammad Golok Jaya<sup>1,2</sup>, Ketut Wikantika<sup>2</sup>, Katmoko Ari Sambodo<sup>3</sup>,  
Armi Susandi<sup>4</sup>

<sup>1</sup>Faculty of Engineering, Halu Oleo University, Indonesia

<sup>2</sup>Center for Remote Sensing, Institute of Technology Bandung (ITB), Indonesia

<sup>3</sup>Indonesia National Institute of Aeronautics and Space (LAPAN)

<sup>4</sup>Meteorology Department, ITB, Indonesia

## ABSTRACT

*This paper was aimed to estimate carbon stocks in South East Sulawesi tropical forest, Indonesia, using Polarimetric Interferometry Synthetic Aperture Radar (PolInSAR). Two coherence Synthetic Aperture Radar (SAR) images of ALOS PALSAR full-polarimetric were used in this research. The research method is forming Random Volume over Ground (RVoG) model from interferometric phase coherence of two Full-Polarimetric ALOS PALSAR which temporal baseline is 46 days. Due to temporal decorrelation, coherence optimization was conducted to produce image with optimum coherences. The result showed that the RVoG forest height and carbon stocks which obtained from height inversion has a positive correlation with ground measurement.*

**Keywords:** Carbon stocks, PolInSAR, ALOS PALSAR, temporal decorrelation, RVoG model

## I. INTRODUCTION

Today, estimation of carbon stocks plays important role in the context of climate change mitigation. Forest layers absorb carbon emission from atmosphere and store it as carbon pool [1]. Indonesia is one of country which has huge tropical forest that contains carbon stocks and gives impact to climate change. Mapping of forest carbon stocks can assist Indonesia to manage mitigation of climate change under the program of Reducing Emission from Deforestation and Forest Degradation (REDD).

Some efforts have been conducted to estimate of Indonesia forest carbon stocks including using optical remote sensing. Due to cloud cover, optical remote sensing system is not optimum in estimation of carbon stocks. Therefore the usage of radar remote sensing system has been widely applied for that purpose. However, radar remote sensor especially its polarimetry has main problem regarding saturation [2]. To solve the problem, development of radar polarimetry interferometry integration leads to overcome the saturation.

The first comprehensive description of Polarimetric Synthetic Aperture Radar Interferometry (PolInSAR) technique was published by Cloude and Papathanassiou in 1998 [3]. Since that time, many researches have been conducted using the PolInSAR for many applications and developments. One of most famous PolInSAR application is biomass and carbon stocks estimation [4], [5], [6], [7].

Indonesia has the first experience of using PolInSAR through INDREX-II airborne campaign in 2004 [5]. The campaign was conducted to develop database aboveground biomass in Kalimantan forest using L- and P-bands in polarimetric and interferometric components by means of Experimental Synthetic Aperture Radar (E-SAR) of the German Aerospace Center (DLR). Radar technology is suitable to map carbon stocks of Indonesia forest environment due to cloud cover, smoke and haze especially in Sumatera, Kalimantan, Sulawesi and Papua. Under the REDD+ program, Indonesia committed to reduce carbon emission 26% (Business As Usual scenario/BAU) and 41% (with international cooperation) by 2020. This effort is officially declared by Indonesia Presidential Act No. 61 Year 2011 about National Movement for Reducing Green House Gases Emission. By year of 2020, the target for reducing carbon emission from forestry and peatland is 0.672 Gt CO<sub>2</sub> using BAU scenario or 1,039 Gt CO<sub>2</sub> through international cooperation [8].

To achieve the purpose, carbon stocks mapping is essential to lead the status that forest become sink or the source of carbon emission. PolInSAR is the promising technique to accelerate mapping of carbon stocks. Tree canopy height in a forest area is important parameter in the estimation of carbon stocks [9]. In some previous studies using allometric models, Diameter at Breast Height (DBH) became one of the critical input on allometric equations to produce the volume of carbon stocks [10], [11]. The main problem with DBH allometric model is that the parameters must be measured directly in the field (semi-empirical method) and the results used in the estimation of carbon stocks. It is time consuming, high cost and becoming not efficient.

Today, the advancement in radar remote sensing, particularly using PolInSAR technique then the measurement of DBH becomes unnecessary [3], [12]. Allometric relationship between tree height and its carbon stock can be obtained through the PolInSAR [13]. The aimed of this paper is to estimate carbon stocks of tropical forest using PolInSAR technique and discuss some aspects regarding the technique.

## II. STUDY AREA

### 2.1 Location

This research was carried out in South East Sulawesi, Indonesia. The location is in Wolasi Tropical Protection Forest in South Konawe Regency ( $4^{\circ}06'10.22''-4^{\circ}12'15.74''S$  and  $122^{\circ}29'2.15''-122^{\circ}30'33.4''E$ ), about 300-700 meter above sea level. Average temperature is 25-34 Celsius degree and annual precipitation is 1,469 millimeter. The topography is mountainous with gradient up to 10-20%. Ten sample plots have been established in location with size of 20x20 square meter. The map of study location is displayed in Figure 1.

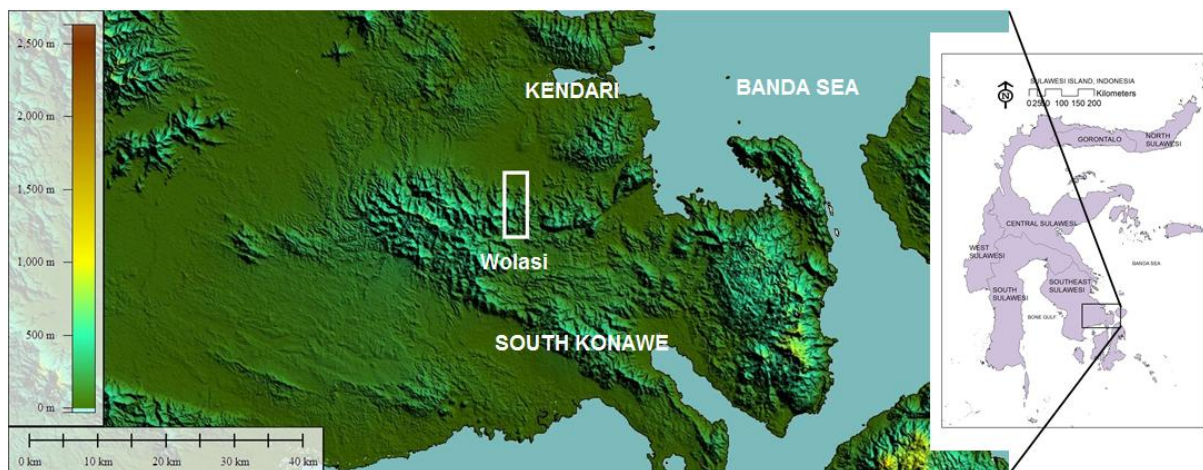


**Figure 1.** Map of study location using SRTM data of South East Sulawesi, Indonesia. White rectangular indicates position of ALOS PALSAR data which used in this study

Vegetation in this location dominated by (in local names) Eha (*Castanopsis buruana*), Batu-Batu (*Ptemandra spp.*), Dange (*Dillenia sp.*) and Ruruhi (*Syzygium spp.*). Some of trees were identified more than 40 years old with diameter more than 30 centimeters. The tree heights between 3 to 35 meter and density is about 200 to 300 trees per hectare. Vegetation condition in the study area and sample of dominated tree species are displayed in Figure 2.



**Figure 2.** Situation of forest in the Study Location (left) and one of dominant tree species (right)

**2.2 SAR Data**

This research conducted using ALOS PALSAR imagery data. Both of the imageries are in full-polarimetric with four polarizations namely HH, HV, VH and VV. Temporal baseline between these images is 46 days. Data characteristics is described in table 1.

**Table 1.** Data Characteristics

Description	Master Image	Slave Image
Center Frequency	1,25 GHz	1,25 GHz
Wavelength	23 cm	23 cm
Polarization	HH, HV, VH, VV	HH, HV, VH, VV
Range Resolution	9.4 m	9.4 m
Azimuth Resolution	3.8 m	3.6 m
Date of acquisition	2 May 2010	17 March 2010
Incidence Angle	23°	21.5°
Pass	Ascending	Ascending
Mode	Single Look Complex (SLC)	SLC

**III. METHODOLOGY**

**3.1 SAR Data Processing**

The key of PolInSAR technique lies in establishment of coherence between two identical images in full-polarizations environment. ALOS PALSAR image from 2 May 2010 acquisition is assigned as master image and 17 March 2010 assigned as slave. Each image was proceed as Sinclair (S2) Matrix. S2 matrix referred to 2x2 dimensions scattering matrix contains all polarizations as displayed in equation (1).

$$S = \begin{bmatrix} S_{HH} & S_{HV} \\ S_{VH} & S_{VV} \end{bmatrix} \tag{1}$$

The S2 matrix contains backscattering properties of the earth objects. Scattering matrix can characterize scatterer wave for any polarization of incidence wave at every image pixel. The elements of the scattering matrix mentioned above is very useful in the analysis of pixels, for example on the classification activity [14]. From the above scattering matrix, the matrix component may be converted into a vector with four elements arranged in the form of the scattering matrix vector, as shown in Equation (2).

$$k = \begin{bmatrix} S_{HH} \\ S_{HV} \\ S_{VH} \\ S_{VV} \end{bmatrix} = [S_{HH} \quad S_{HV} \quad S_{VH} \quad S_{VV}]^T \tag{2}$$

Since backscatter of  $S_{HV} = S_{VH}$ , according to the principle of reciprocity in polarimetry, then Equation (2) can be transformed into Equation (3).

$$k = [S_{HH} \quad \sqrt{2}S_{HV} \quad S_{VV}]^T \tag{3}$$

Another famous form of the Equation (2) is Pauli basis target vector [Cloude and Pottier, 1996; Richards, 2009] as shown in Equation (4).

$$k_p = \frac{1}{\sqrt{2}} [S_{HH} + S_{VV} \quad S_{HH} - S_{VV} \quad S_{HV} + S_{VH} \quad j(S_{HV} - S_{VH})]^T \tag{4}$$

For backscattering, in which the two cross-polar terms are equal, the Equation (4) can be reduced to Equation (5).

$$k_p = \frac{1}{\sqrt{2}} [S_{HH} + S_{VV} \quad S_{HH} - S_{VV} \quad 2S_{HV}]^T \tag{5}$$

From Equation (5), for co-registration of two full-polarimetric SAR coherent image, then can be formed the Hermitian 6x6 [T6] matrix as shown in Equation (6).

$$[T_6] = \langle \begin{bmatrix} k_1 \\ k_2 \end{bmatrix} [k_1^* \quad k_2^*] \rangle = \begin{bmatrix} [T_{11}] & [\Omega_{12}] \\ [\Omega_{12}]^* & [T_{22}] \end{bmatrix} \tag{6}$$

Where  $\langle \rangle$  represented multi-looking operator,  $*$  is Hermitian transformation,  $k_1$  and  $k_2$  are 3D Pauli scattering vectors.  $[T_{11}]$  and  $[T_{22}]$  are standard Hermitian coherency matrix contained full-polarimetric information from each full-polarimetric image.  $[\Omega_{12}]$  states new complex matrix in 3x3 dimension, which contains not only polarimetric information, but also interferometric phase between polarimetric channel in the coherent pair images [14]. The T6 matrix then be proceed to estimate the coherence of interferogram and to produce the RVoG model.

### 3.2 Field Data Processing

Tree height and Diameter at Breast Height (DBH) for each tree were measured for all sample plots. To calculate biomass volume from these two parameters, Allometric Equation formula from Indonesia Agency for Forestry Research and Development was used as shown in Equation (7) [15].

$$V = 0.25\pi\left(\frac{D}{100}\right)^2 HF, \tag{7}$$

Where:

$\pi = 3.14$

D = DBH (centimeter)

H = Tree Height (meter)

F = Tree dimension factor 0.6

The result from Equation (7) then convert to carbon stocks volume using Inter-governmental Panel on Climate Change (IPCC) formula [1] as shown in Equation (8).

$$C=0.47*V \tag{8}$$

Where C states the carbon stocks volume.

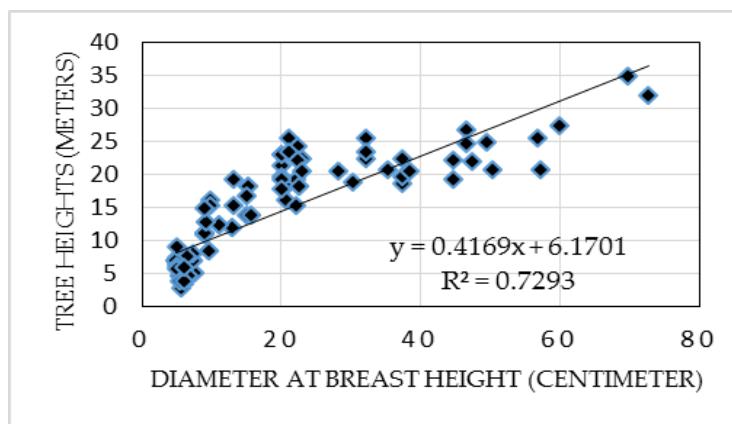


**Figure 3.** Correlation between diameter at breast height (in centimeters) dan tree heights (in meters) from field survey

Figure 3 above displays us correlation between diameter at breast height (DBH) dan tree heights from field survey. It showed that the correlation ( $R^2$ ) from these two variables is 0.73

## IV. RESULT AND DISCUSSION

Vegetation type will determine the radar frequency which used in carbon stocks estimation. For example, to estimate carbon stocks in grass vegetation, the X-band frequency is more suitable than the L band or C band. This due to radar backscatter in the X band frequency are more optimum interaction with grass vegetation cover. For shrubs plant or herbaceous plant, the X-band frequency is not suitable to be used because the vegetation structure becomes more complex, then it suggested to use the C-band [7], [14].

In order to understand the characteristics of the vegetation, it is important to select proper frequencies that can penetrate vegetation and produce backscatter optimally. For the high-level vegetation including on remote forest

area or primary forest, it is suggested to use L-band frequencies and even P-band [14], [16], [17]. For more penetration, the usage of HV polarization can provide better information than using HH [18], [19].

Two coherence SAR images from different time and different position of acquisition were proceed as master and slave as displayed in Figure 4 in Red Green Blue (RGB) Pauli composition.

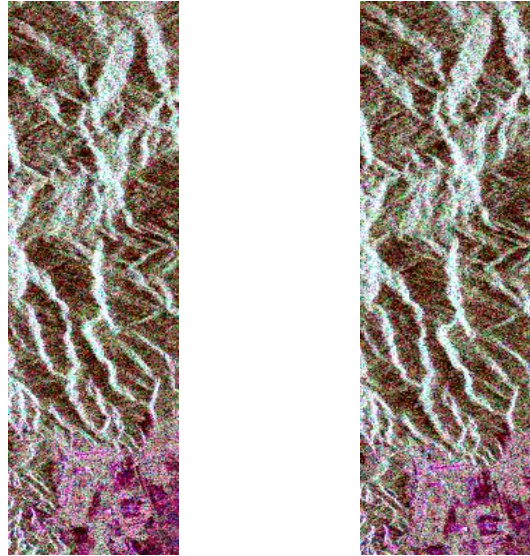


**Figure 4.** Pairs of ALOS PALSAR images in RGB Pauli: left image is master and right image is slave

#### ***PolInSAR***

Since proposed by Cloude and Papathanassiou (1998) [3], PolInSAR technique has undertaken many advancements through the improvements in analysis of temporal decorrelation, coherence optimization, improvement of Random Volume over Ground model, inversion height of vegetation and improvements in the estimation of ground topography [6], [9], [12] and application of PolInSAR using dual polarization [20], [21].

In the perspective of measuring carbon stocks, Interferometry SAR (InSAR) can measure or determine the phase center of the whole of a signal on a pixel but will not be able to distinguish the location of the point scattering that located in the canopy or at ground topography. This problem can be solved through the application of polarization on the scope of interferometry (PolInSAR) [3].

Polarimetry components is sensitive to the shape and orientation of the object, while interferometry sensitive to the spatial distribution and height of objects. Thus PolInSAR has ability to identify the mechanism of scattering in a medium by applying a phase difference at different polarizations [3]. Therefore PolInSAR not only use different phases, but also amplitude of the complex coherence interferometry to determine the vertical structure of vegetation volume by separating location between the phase center on a variety of different polarizations [4], [7], [14], [22].

A PolInSAR system works by two polarimetric image data derived from two different observation positions that generate complex polarimetric interferometric coherency as defined [14]

$$\gamma = |\gamma|e^{j\Delta\phi} = \frac{\langle k_1 k_2^* \rangle}{\sqrt{\langle k_1 k_1^* \rangle \langle k_2 k_2^* \rangle}} \quad (9)$$

$k_1$  and  $k_2$  is the vector of the target in the image that will be interferenced, because both vectors containing the information required to establish the interferometric image for all combinations of polarization [3].

For two coherent SAR images, interferometric phase difference is formulated as follows

$$\Delta\phi = \Delta\phi_{baseline} + \Delta\phi_{polarization} + \Delta\phi_{pixel} + \Delta\phi_{others} \quad (10)$$

Eq. 10 shows us that the coherence between two images are depend on interferometric baseline used, polarization chosen, changes in the specific region of the image of interest and other factors, such as noise [14].

**Coherence Optimization**

The main problem in PolInSAR is temporal decorrelation [7], [13], [14]. Temporal decorrelation will lead to uncertainty in formation of interferogram. It cannot be avoided in repeat pass mode of SAR system [14]. To reduce the impact of temporal decorrelation, coherence optimization was conducted. From eq. 9, the complex polarimetric interferometric coherence can be written as  $\gamma(w_1, w_2)$  as a function of the polarization of the two images. It can be then written as [7]:

$$\gamma(w_1, w_2) = \frac{w_1^{*T} \Omega_{12} w_2}{\sqrt{(w_1^{*T} T_{11} w_1)(w_2^{*T} T_{22} w_2)}} \tag{11}$$

The modulus of  $\gamma(w_1, w_2)$  indicates the degree of correlation between two images, while its argument corresponds to interferometric phase difference or interferogram [7].

The dependency of the interferometric coherence on the polarization formed by  $w_1$  and  $w_2$  leads us to consider the combination of polarizations yield the highest coherence [Lee and Pottier, 2009]. In order to solve the polarimetric interferometric optimization problem, Cloude and Papathanassiou [4] proposed a method maximizing the complex Lagrangian function L which defined as:

$$L = w_1^{*T} \Omega_{12} w_2 + \lambda_1 (w_1^{*T} T_{11} w_1 - C_1) + \lambda_2 (w_2^{*T} T_{22} w_2 - C_2) \tag{12}$$

Where

$C_1$  and  $C_2$  are constants

$\lambda_1$  and  $\lambda_2$  are the Lagrangian multipliers introduced in order to maximize the modulus of the numerator of Equation (12) while keeping the denominator constant [7].

Figure 5 below showed the results of three optimum of complex polarimetry interferometric coherence from three Eigen vectors.

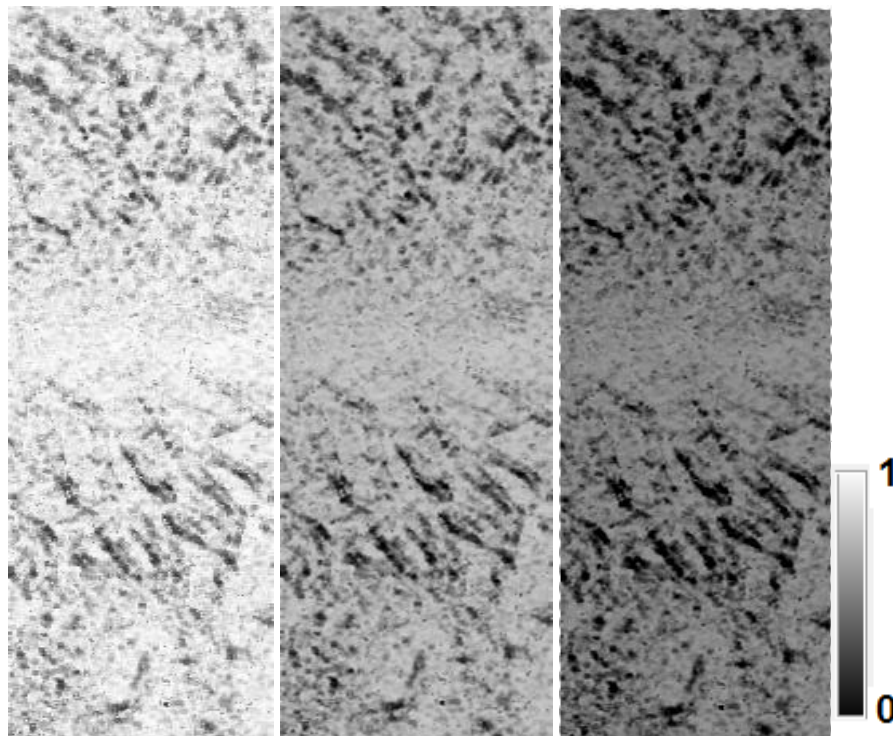


**Figure. 5** Results of optimization of complex polarimetry interferometric coherence: OPT\_1 (left), OPT\_2 (middle) and OPT\_3 (right)

Coherence value will be zero (0) for minimum called incoherence (black colour) and one (1) for maximum, called fully coherence (white colour). Figure 5 (left) is identified as the best coherence since the histogram near to one. The optimum coherence value becomes one on the fields but drops down in the forested area because of the residual volume component which cannot be removed [12].

**RVOG Heights Model**

The RVoG model is physical interpretation of forest vegetation [4], [12]. RVoG model consists of two layers to model random volume of scattered particles, which represents the canopy layer over a ground surface as shown in Equation (13). This procedure so-called forest height inversion [4].

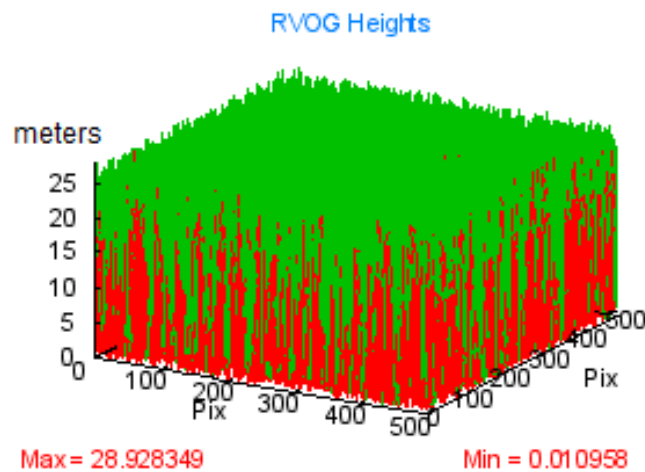
$$\tilde{\gamma}_v = \exp(ik_z z_0) \frac{\tilde{\gamma}_{v0}^{1+m}}{1+m} \tag{13}$$

$k_z z_0 = \varphi_0$  is associated with the topographic phase  $z_0$  while  $k_z$  is the vertical wavenumber and  $m$  is the amplitude ratio of effective ground-to-volume calculated for attenuation through volume.  $\tilde{\gamma}_{v0}$  states volume decorrelation which caused by the absence of ground layer. Equation (13) can be expanded as Equation (14).

$$\tilde{\gamma}_v = \exp(ik_z z_0) \frac{\int_0^{h_v} \exp(ik_z z') \exp\left(\frac{2\sigma z'}{\cos\theta_0}\right) dz'}{\int_0^{h_v} \exp\left(\frac{2\sigma z'}{\cos\theta_0}\right) dz'} \tag{14}$$

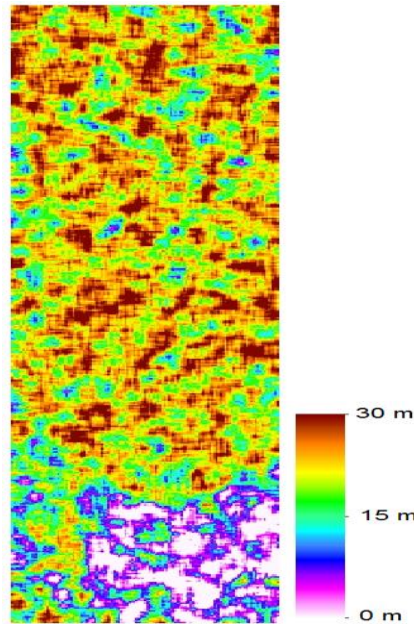
Where  $\sigma$  is the average coefficient differentiator and  $\theta$  is the incidence angle.  $k_z$  is calculated from  $\theta$  (incidence angle), the difference between the two incidence angle ( $\Delta\theta$ ) and wavelength  $\lambda$ , as seen in the equation (15).

$$k_z = \frac{4\pi\Delta\theta}{\lambda \sin\theta} \text{ radians/meter} \tag{15}$$



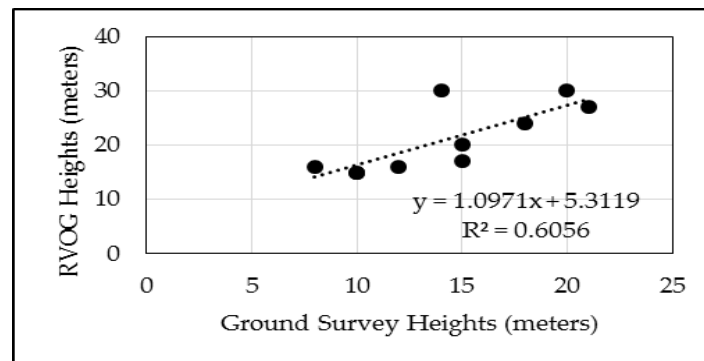
**Figure 6.** RVoG Height Model from PolINSAR

Figure 6 displays the RVoG model resulted from PolInSAR. From this model we can generate tree height distribution map as displayed on Figure 7.



**Figure 7** Tree forest height map

The map displays tree height distributed from 0 to 30 meters which 10-30 meters heights dominated the study area. The result need to be correlated to the ground survey. From 10 sample plots of ground measurement we obtained correlation between tree heights and RVoG heights as displayed in Figure 8 ( $R^2=0.6056$ ).



**Figure 8** Correlation between ground survey and RVoG Heights (in meters)

### ***Carbon Stocks Estimation***

To estimate carbon stocks, allometric equation was used to build correlation between physical dimensions of tree stand with the biomass. Mette (2006) [13] proposed an allometric equation for direct estimation of biomass from tree height.

$$B = 0.925 \times 1.66 \times h^{1.58} \quad (16)$$

Where B is biomass (kilograms) and h is tree height (meters). This equation, of course, will not suitable for all types of forest (i.e tropical forest), but it can be seen as the best approach for estimating the biomass. From equation (16), carbon stocks volume in the study area range between 250 to 350 t ha<sup>-1</sup>.

## **V. CONCLUSION**

The PolInSAR technique as conducted in this research has showed us the beneficial of integration radar polarimetry and interferometry to estimate carbon stocks in tropical forest. The technique helped us to estimate tree height through RVoG model without disturbance by saturation. However, the RVoG model is depend on coherency. Coherence optimisation has to be conducted to maximize the coherence due to temporal decorrelation. Temporal decorrelation caused by 46 days temporal baseline may still effect to the RVoG model. This effect can be observed through correlation between tree height which is resulted from ground measurement and RVoG model where  $R^2=0.6056$ .

## ACKNOWLEDGEMENT

We would like thanks to Professor M. Shimada from Japan Aerospace and Exploration Agency (JAXA) who provided ALOS PALSAR Full-Polarimetric that used in this research. Also thanks to our colleagues at Faculty of Forestry Halu Oleo University, Indonesia for conducting field survey.

## REFERENCES

- [1]. IPCC (Inter-Governmental Panel on Climate Change), 2007. "The Carbon Cycle and Atmospheric Carbon Dioxide Content", *Coordinating Lead Author*: I.C. Prentice, *Lead Authors*: G.D. Farquhar, M.J.R. Fasham, M.L. Goulden, M. Heimann, V.J. Jaramillo, H.S. Keshgí, C. Le Quéré, R.J. Scholes, D.W.R. Wallace, *Contributing Authors*: D. Archer, M.R. Ashmore, O. Aumont, D. Baker, M. Battle, M. Bender, L.P. Bopp, P. Bousquet, K. Caldeira, P. Ciais, P.M. Cox, W. Cramer, F. Dentener, I.G. Enting, C.B. Field, P. Friedlingstein, E.A. Holland, R.A. Houghton, J.I. House, A. Ishida, A.K. Jain, I.A. Janssens, F. Joos, T. Kaminski, C.D. Keeling, R.F. Keeling, D.W. Kicklighter, K.E. Kohfeld, W. Knorr, R. Law, T. Lenton, K. Lindsay, E. Maier-Reimer, A.C. Manning, R.J. Matear, A.D. McGuire, J.M. Melillo, R. Meyer, M. Mund, J.C. Orr, S. Piper, K. Plattner, P.J. Rayner, S. Sitch, R. Slater, S. Taguchi, P.P. Tans, H.Q. Tian, M.F. Weirig, T. Whorf, A. Yool, *Review Editors*: L. Pitelka, A. Ramirez Rojas
- [2]. Moreira, A., Papathanassiou, K., Krieger, G., 2002, "Polarimetric SAR Interferometry with a Passive Polarimetric Micro-Satellite Concept", Institute of Radio Frequency Technology and Radar Systems, German Aerospace Center (DLR)
- [3]. Cloude, S.R and Papathanassiou, K., 1998. "Polarimetric SAR Interferometry", IEEE Transactions on Geoscience and Remote Sensing, Vol. 36 No. 5, pp. 1551-1565, September 1998
- [4]. Cloude, S.R and Papathanassiou, K., 2003. "Three-stage inversion process for Polarimetric SAR Interferometry", IEE Proc-Radar Sonar Navigation, 150: 125-134
- [5]. Hajnsek, I., Kugler, F., Papathanassiou, K., Horn, R., Schieber, R., Moreira, A., Hoekman, D., Davidson, M. 2005. "INDREX II – Indonesian airborne radar experiment campaign over tropical forest in L- and P- band: first results", Proceedings of Geoscience and Remote Sensing Symposium 2005 (IGRASS 2005) Page(s): 4335-4338, July 25-29, 2005, Seoul, South Korea.
- [6]. Florian, K., Papathanassiou K., Hajnsek, I. and Dirk, H., 2006. "Forest height estimation in tropical rain forest using Pol-Insar techniques", German Aerospace Center (DLR), IEEE 0-7803-9510-7/06
- [7]. Lee, Jong-Sen and Pottier, Eric, 2009. "Polarimetric Radar Imaging from Basics to Applications", CRC Press, ISBN 978-1-4200-5497-2
- [8]. Indonesia Secretary of Cabinet, 2012. "Indonesia Presidential Act No. 61 Year 2011: National Movement for Reducing Green House Gases Emission".
- [9]. Mette, T., Papathanassiou, K.P., Hajnsek, I., Zimmermann, R. 2003. "Forest Biomass Estimation using Polarimetric SAR Interferometry".
- [10]. Chave, J., Andalo, C., Brown, S., Cairns, M.A., Chambers, JQ., Eamus, D., Fo lster, H., Fromard, F., Higuchi, N., Kira, T., Lescure, JP., Nelson, BW., Ogawa, H., Puig, H, Rie'ra, B., Yamakura, T., 2005. "Tree allometry and improved estimation of carbon stocks and balance in tropical forests", *Ecosystem Ecology, Oecologia* (2005) 145: 87–99, DOI 10.1007/s00442-005-0100-x
- [11]. Saatchi, S., Marlier, M., Chazdon R.L., Clark, DB., Russell, AE., 2011. "Impact of spatial variability of tropical forest structure on radar estimation of aboveground biomass", *Remote Sensing of Environment*, doi:10.1016/j.rse.2010.07.015
- [12]. Papathanassiou, K. and Cloude, S.R., 2001. "Single base-line Polarimetric SAR Interferometry", IEEE Transactions on Geoscience and Remote Sensing, Vol. 39 No. 11, pp. 2352-2363
- [13]. Mette, Tobias, 2006. "Forest Biomass Estimation from Polarimetric SAR Interferometry", Dissertation, Technischen Universität München
- [14]. Richards, J. A., 2009. "Remote Sensing with Imaging Radar, Signals and Communication Technology", ISBN: 978-3-642-02019-3, Springer
- [15]. Badan Penelitian dan Pengembangan Kehutanan (Indonesia Agency for Forestry Research and Development) , 2013. Pedoman Penggunaan Model Allometrik untuk Pendugaan Biomass dan Stok Karbon Hutan di Indonesia", Peraturan Kepala Badan Penelitian dan Pengembangan Kehutanan No. P.01/VIII-P3KR/2012, Kementerian Kehutanan Republik Indonesia, ISBN: 978-979-3145-97-6
- [16]. Kurvonen, L., Pulliainen, J., and Hallikainen, M., 1999. "Retrieval of biomass in boreal forest from multitemporal ERS-1 and JERS-1 SAR images", IEEE Transactions on Geoscience and Remote Sensing, 37, pp. 198-205
- [17]. Lee, S., Kugler, F., Papathanassiou, K., Hajnsek, I., 2010. "Polarimetric SAR Interferometry for Forest Application at P-Band: Potentials and Challenges", German Aerospace Center (DLR), Institute of Radio Frequency Technology and Radar System (DLR-HR)
- [18]. Luckman, A.J., 1997. "Texture in airborne SAR imagery of tropical forest and its relationship to forest regeneration stage", *International Journal of Remote Sensing*, 18, pp. 1333-1349
- [19]. Le Toan, T., Quegan, S., Davidson, M.W.J., Baltzer, H., Paillou, P., Papathanassiou, K., Plummer, S., Rocca, F., Saatchi, S., Shugart, H., Ulander, L. 2011, "the BIOMASS Mission : Mapping global forest biomass to better understand the terrestrial carbon cycle", *Remote Sensing of Environment* 115 (2011) 2850-2860
- [20]. Fu, W.X., Guo, H.D., Xie, C., Lu, Y.C., and Li, X.W., 2014. "Forest height inversion using dual-pol polarimetric SAR interferometry", 35<sup>th</sup> International Symposium on Remote Sensing of Environment (ISRSE35), IOP Conf. Series: Earth and Environmental Science 17 (2014) 012072, IOP Publishing, DOI: 10.1088/1755-1315/17/1/012072
- [21]. Minh, N.P., and Zou, B, 2013. "A novel algorithm for forest height estimation from Polinsar image", *International Journal of Signal Processing, Image Processing and Pattern Recognition*, Vol. 6, No. 2, April 2013
- [22]. Wenxue, F., Huadong, G., Xinwu, L., Bangsen, T. and Zhongchang, S, 2015. "Extended Three-Stage Polarimetric SAR Interferometry Algorithm by Dual-Polarization Data", IEEE Transactions on Geoscience and Remote Sensing, DOI: 10.1109/TGRS.2015.2505707